

Relevance Attack on Detectors

Sizhe Chen^a, Fan He^a, Xiaolin Huang^{a,*}, Kun Zhang^b

^a*Department of Automation, the Institute of Medical Robotics, and the MOE Key Laboratory of System Control and Information Processing, Shanghai Jiao Tong University, 800 Dongchuan Road, Shanghai, 200240, P.R. China.*

^b*Philosophy Department, and Machine Learning Department, Carnegie Mellon University, 5000 Forbes Ave, Pittsburgh, PA 15213, United States*

Abstract

This paper focuses on high-transferable adversarial attacks on detectors, which are hard to attack in a black-box manner, because of their multiple-output characteristics and the diversity across architectures. To pursue a high attack transferability, one plausible way is to find a common property across detectors, which facilitates the discovery of common weaknesses. We are the first to suggest that the relevance map from interpreters for detectors is such a property. Based on it, we design a Relevance Attack on Detectors (RAD), which achieves a state-of-the-art transferability, exceeding existing results by above 20%. On MS COCO, the detection mAPs for all 8 black-box architectures are more than halved and the segmentation mAPs are also significantly influenced. Given the great transferability of RAD, we generate the first adversarial dataset for object detection and instance segmentation, i.e., Adversarial Objects in COntext (AOCO), which helps to quickly evaluate and improve the robustness of detectors.

Keywords: adversarial attack, attack transferability, black-box attack, relevance map, interpreters, object detection.

*Corresponding author

Email addresses: sizhe.chen@sjtu.edu.cn (Sizhe Chen), hf-inspire@sjtu.edu.cn (Fan He), xiaolinhuang@sjtu.edu.cn (Xiaolin Huang), kunz1@cmu.edu (Kun Zhang)

1. Introduction

Adversarial attacks [1, 2, 3, 4, 5, 6] have revealed the fragility of Deep Neural Networks (DNNs) by fooling them with elaborately-crafted imperceptible perturbations. Among them, the black-box attack, i.e., attacking without knowledge of their inner structure and weights, is much harder, more aggressive, and closer to real-world scenarios. For classifiers, there exist some promising black-box attacks [7, 8, 9, 10, 11, 12]. It is also severe to attack object detection [13] in a black-box manner, e.g., hiding certain objects from unknown detectors [14]. By that, life-concerning systems based on detection such as autonomous driving and security surveillance would be greatly influenced.

To the best of our knowledge, no existing attack is specifically designed for black-box transferability in detectors, because they have multiple-outputs and a high diversity across architectures. In such situations, adversarial samples do not transfer well [15], and most attacks only decrease mAP of black-box detectors by 5 to 10% [16, 17, 18]. To overcome this, we propose one plausible way to find common properties across detectors inspired by our AoA attack [12], which facilitates the discovery of common weaknesses. Based on them, the designed attack can threaten variable victims.

In this paper, we adopt the relevance map from DNN interpreters as a common property, on which different detectors have similar interpretable results, as shown in Fig. 1. Based on relevance maps, we design a Relevance Attack on Detectors (RAD). RAD focuses on suppressing the relevance map rather than directly attacking the prediction as in existing works [16, 17, 19]. Because the relevance maps are quite similar across models, those of black-box models are influenced and misled as well in attack, leading to great transferability. Although some works have adopted the relevance map as an indicator or reference of success attacks [20, 21, 12, 22], there is no work to directly attack the relevance maps of detectors to the best of our knowledge.

In our comprehensive evaluation, RAD achieves the state-of-the-art transferability on 8 black-box models for COCO) dataset [23], nearly halving the

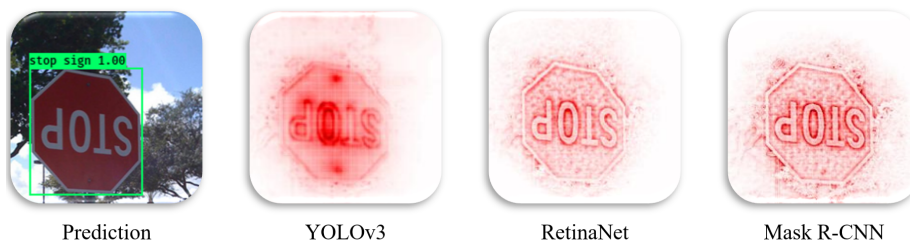


Figure 1: Relevance maps for models with different architectures. Three models not only predict the “stop sign” right, but also share similar relevance maps.

detection mAP. Interestingly, the adversarial samples of RAD also greatly influence the performance of instance segmentation, even only detectors are attacked. Given the high transferability of RAD, we create Adversarial Objects in Context (AOCO), the first adversarial dataset for object detection and instance segmentation. AOCO contains 10K samples that significantly decrease the performance of black-box models for detection and segmentation. AOCO may serve as a benchmark to test the robustness of a DNN or improve it by adversarial training.

Contributions

- We propose a novel attack framework on relevance maps for detectors. We extend DNN interpreters to detectors, find out the most suitable nodes to attack by relevance maps, and explore the best update techniques to increase the transferability.
- We evaluate RAD on 8 black-box models and find its state-of-the-art transferability, which exceeds existing results by above 20%. Detection mAPs are more than halved, invalidating the state-of-the-art detectors to a large extent.
- By RAD, we create the first adversarial dataset for object detection and instance segmentation, i.e., AOCO. As a potential benchmark, AOCO is generated from COCO and contains 10K high-transferable samples. AOCO helps to quickly evaluate and improve the robustness of detectors.

2. Related Work

Since [1], there have been lots of promising adversarial attacks [2, 3, 4]. Generally, they fix the network weights and change the input slightly to optimize the attack loss. The network then predicts incorrectly on adversarial samples with high confidence. [7, 24] find that adversarial samples crafted by attacking a white-box surrogate model may transfer to other black-box models as well. Input modification [10, 20, 11] or other optimization ways [9, 11] are validated to be effective in enhancing the transferability.

[16] extends adversarial attacks to detectors. It proposes to attack on densely generated bounding boxes. After that, losses about localization and classification are designed [17] for attacking detectors. [25] and [19] propose to attack detectors in a restricted area. Existing works achieve good results in white-box scenarios but are not specifically designed for transferability. The adversarial impact on black-box models is quite limited, i.e., a 5 to 10% decrease from the original mAP, even when two models only differ in backbone [16, 17, 18]. [26] discusses black-box attacks towards detectors based on queries rather than the transferability as we do. The performance is satisfactory, but it requires over 30K queries, which is easy to be discovered by the model owner. Besides, physical attacks on white-box detectors are also feasible [27, 28, 29, 30].

For great transferability, we propose to attack relevance maps, which are calculated by DNN interpreters [31, 32, 33]. They are originally developed to interpret how DNNs predict and help users gain trust in them. Specifically, they display how the input contributes to a certain node output in a pixel-wise manner. Typical works include Layer-wise Relevance Propagation (LRP) [34], Contrastive LRP [35] and Softmax Gradient LRP (SGLRP) [36]. These methods encourage the reference of relevance maps in attack [20, 21, 12, 22], and also inspire us. However, none of them attack relevance maps for detectors.

RAD differs from [37, 38] in the goal. RAD misleads detectors by suppressing relevance maps. [37] misleads the relevance maps while keeping the prediction unchanged. [38] also misleads DNNs, but it keeps the relevance maps unchanged.

3. Relevance Attack on Detectors

We propose an attack specifically designed for black-box transferability, named Relevance Attack on Detectors (RAD). RAD suppresses multi-node relevance maps for several bounding boxes. Since the relevance map is commonly shared by different detectors as shown in Fig. 1, attacking it in the white-box surrogate model achieves a high transferability towards black-box models. In this section, we first provide a high-level overview of RAD, and analyze the potential reasons for its transferability. Then we thoroughly discuss three crucial concrete issues in RAD.

- In Section 3.3, we extend existing classifier interpreters to detector ones.
- In Section 3.4, we introduce the proper nodes to attack by RAD.
- In Section 3.5, we explore the suitable techniques to update samples.

3.1. What is RAD?

We present the framework of RAD in Fig. 2. Initialized by the original sample x_0 , the adversarial sample x_k in the k^{th} iteration is forward propagated in the surrogate model, getting the prediction $f(x_k)$. Current attacks generally suppress the prediction values of all attacked output nodes in T . In contrast, RAD suppresses the corresponding relevance map $h(x_k, T)$. To restrain that, gradients of $h(x_k, T)$ back propagate to x_k , which is then modified to x_{k+1} .

Notably, RAD is a complete framework to attack detectors, and its components require special design. Besides the calculation of relevance maps of detectors, other components in RAD, e.g., the attacked nodes or the update techniques, also need a customized analysis. The reason is that no existing work directly attacks the relevance of detectors, and the experience in attacking predictions is not applicable here. For example, [13] emphasizes classification loss and localization loss equally, but the former is validated to be significantly better in attacking the relevance in Section 3.4.

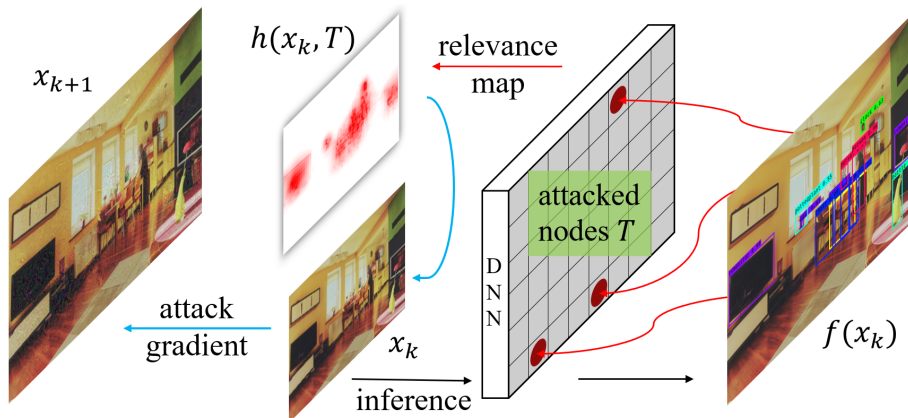


Figure 2: Framework of RAD. x_k is the sample in iteration k and $f(x_k)$ is the network prediction for it. $h(x_k, T)$ stands for the relevance map for all attacked nodes in T . RAD works by repeating processes denoted by “black”, “red” and “blue” arrows in turn.

3.2. Why RAD Transfers?

RAD’s transferability comes from the attack goal: changing the common properties, i.e., the relevance maps. As shown in Fig. 3, the relevance maps are clear and structured for the original sample in both detectors. After RAD, the relevance maps are induced to be meaningless without a correct focus, leading to wrong predictions, i.e., no or false detection. Because relevance maps transfer well across models, those for black-box detectors are also significantly influenced, causing a great performance drop, which is illustrated visually in Section 4.2.

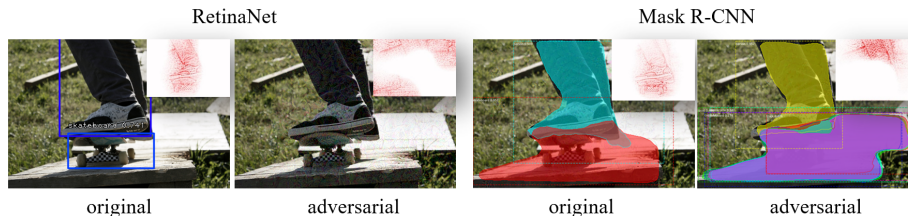


Figure 3: RAD’s transferability origins from the change of relevance maps. The image contains a person and a skateboard. By attacking on relevance maps, both surrogate models make extremely confusing predictions.

RAD also attacks quite “precisely”, i.e., the perturbation pattern is signifi-

cantly focused on distinct areas and has a clear structure as shown in Fig. 4. That is to say, RAD accurately locates the most discriminating parts of a sample and concentrates the perturbation on them, leading to a great transferability when the perturbations are equally bounded.

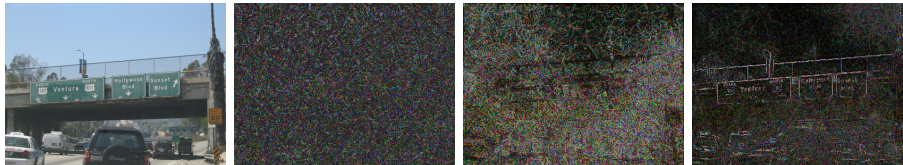


Figure 4: The original image and the adversarial perturbations ($\times 5$ in magnitude for demonstration) generated by Dfool [25], DAG [16], and RAD (from left to right)

3.3. What is the Relevance Maps for Detectors?

We analyze the potential of RAD above, below we make it feasible by addressing three crucial issues. To conduct the relevance attack, we first need to know the relevance maps for detectors.

Currently, there exist lots of interpreters to calculate the relevance maps for classifiers as described in Section 2, but none of them are suitable for detectors. We take SGLRP [36] as an example to explain this and then to modify because it excels in discriminating against irrelevant regions of a certain target node.

SGLRP visualizes how the input contributes to one output node in a pixel-wise way by back-propagating the relevance from the output to the input based on Deep Taylor Decomposition (DTD) as illustrated in Appendix A. $R^{(L)}$ is the initial relevance in the output layer L and its n^{th} component is calculated as

$$R_n^{(L)} = \begin{cases} y_n (1 - y_n) & n = t, \\ -y_n y_t & n \neq t, \end{cases} \quad (1)$$

where y_n is the predicted probability of class n , and y_t is that for the single-node target t . The pixel-wise relevance map $h(x, t)$ for the single-node target t is calculated by back propagating the relevance R from the final layer to the input following rules specified in [36].

In detectors, we need the pixel-wise contributions from the input to m bounding boxes. This multi-node relevance map could not be directly calculated by (1), so we naturally modify SGLRP as

$$R_n^{(L)} = \begin{cases} y_n (1 - y_n) & n \in T, \\ -\frac{1}{m} y_n \sum_{i=1}^m y_{t_i} & n \notin T, \end{cases} \quad (2)$$

where y_{t_i} is the predicted probabilities for one target node t_i . T is the set containing all target nodes $\{t_1, t_2, \dots, t_m\}$. With iNNvestigate Library [39] to implement Multi-Node SGLRP and Deep Learning platforms supporting auto-gradient, the gradients from RAD loss $L_{\text{RAD}}(x) = h(x, T)$ to sample x could be obtained according to the calculation rules of relevance maps in Appendix A.

We illustrate the difference between SGLRP and our Multi-Node SGLRP in Fig. 5. SGLRP only displays the relevance map for one bounding box, e.g., “TV”, “chair” and “bottle”. Multi-Node SGLRP, in contrast, visualizes the overall relevance.



Figure 5: Difference between relevance maps from SGLRP and Multi-Node SGLRP. The relevance maps are for YOLOv3 [40].

3.4. Where to Attack?

Besides the calculation of relevance maps, it is also important to choose a proper node-set T to attack. Specifically, we need to select certain bounding boxes and the corresponding output nodes for RAD.

Heuristically, the most “obvious” bounding boxes are desired to be eliminated, so we select the bounding boxes with the highest confidence, following [16]. Concretely, it is feasible to *statically* choose m bounding boxes to attack in each iteration, or *dynamically* attack all bounding boxes whose confidence exceeds a threshold. In our evaluation, the two strategies differ a little in performance

and are not sensitive to hyper-parameter as demonstrated in Appendix B. This shows that RAD does not require a sophisticated tuning of parameters, which is user-friendly. In our following experiments, we statically attack $m = 20$ nodes.

After selecting bounding boxes, we could attack their size, leading them to shrink; or their localization, leading them to shift; or their confidence, leading them to be misclassified. To adopt the best strategy, we conduct a toy experiment by attacking YOLOv3 [40], denoted as M2, and other models are specified in Table 3. Given the results in Table 1, the classification loss induces a better black-box transferability. This may be because detectors generally include a pre-trained classification as the feature extractor, and relevance maps are believed to be an indicator of successful attacks [20, 21].

Table 1: Detection mAP in RAD with different attacked nodes

Strategy	M1	M2	M3	M4	M5	M6	M7	M8	M9
No Attack	29.3	33.4	38.1	40.7	42.1	42.5	45.7	46.9	53.9
Size	26.0	14.7	31.9	32.5	35.6	35.4	38.6	40.0	47.8
Local.	22.8	6.4	27.4	28.1	31.7	30.8	34.4	35.9	45.1
Class.	18.1	1.2	19.9	20.5	24.3	22.6	26.4	28.2	39.9

3.5. How to Update?

By the relevance map $h(x, T)$ for certain attacked nodes T , we are able to attack, i.e., update the original sample to become adversarial with the guidance of the attack gradients $g(x)$ as

$$g(x) = \frac{\partial L_{\text{RAD}}(x)}{\partial x} = \frac{\partial h(x, T)}{\partial x}. \quad (3)$$

Some update techniques are validated to be effective for enhancing the transferability in classification. For example, Scale-Invariant (SI) [11] proposes to average the attack gradients by scale copies of the samples as

$$g_{\text{si}}(x) = \frac{1}{k} \sum_{i=0}^k g(x/2^i). \quad (4)$$

Besides SI, Diverse Input (DI) [10], Translation-Invariant (TI) [20] are also promising in classification. We are curious about whether they also work well in object detection. To explore this, we adopt these techniques in RAD as the setting suggested by their designers (see Appendix C). From the results in Table 2, we discover that SI is quite effective, further decreasing the mAP from the baseline to a large extent. Accordingly, we adopt (4) to update in RAD.

Table 2: Detection mAP in RAD with different update techniques

Technique	M1	M2	M3	M4	M5	M6	M7	M8	M9
None	18.1	1.2	19.9	20.5	24.3	22.6	26.4	28.2	39.9
DI	18.1	1.0	19.9	20.5	23.9	22.4	26.3	27.9	39.6
TI	17.0	2.4	20.8	20.8	25.2	23.0	27.9	29.7	41.5
SI	14.6	0.7	16.3	17.0	20.4	19.1	22.3	23.8	35.0

With the calculated gradient, we update the sample as

$$x_{k+1} = \text{clip}_\varepsilon \left(x_k - \alpha \frac{g_{\text{si}}(x_k)}{\|g_{\text{si}}(x_k)\|_1/N} \right), \quad (5)$$

where α stands for the step length. x is ℓ_∞ -norm bounded by ε from the original sample in each iteration as in [10, 20, 11]. Gradient $g(x)$ is normalized by its average ℓ_1 -norm, i.e., $\|g(x)\|_1/N$ to prevent numerical errors and control the degree of perturbations. N is the dimension of the image, i.e., $N = \text{height} \times \text{width} \times \text{channel}$. Division by N is necessary because ℓ_1 -norm sums all components of the tensor x , which is too large as a normalization factor. We do not adopt the mainstream *sign* method because it is not suitable to generate small perturbations as shown in other attacks in detectors [16].

4. Experiments

In this section, we evaluate the performance of RAD, especially its transferability. The results are presented visually and numerically. In comprehensive evaluation, RAD achieves great transferability across models and even tasks.

4.1. Setup

Our experiments are based on Keras [41], Tensorflow [42] and PyTorch [43] in 4 NVIDIA GeForce RTX 2080Ti GPUs. Library iNNvestigate [39] is used to implement Multi-Node SGLRP.

We conduct experiments on MS COCO 2017 dataset [23], which is a large-scale benchmark for object detection, instance segmentation, and image captioning. For a fair evaluation, we generate adversarial samples from all 5K samples in its validation set and test several black-box models on their mAP, a standard measure in many works [44, 45].

All attacks are conducted with the step length $\alpha = 2$ for 10 iterations and the perturbation is ℓ_∞ -bounded in $\varepsilon = 16$ to guarantee the imperceptibility as in [20] if not particularly specified. To validate that the mAP drop comes from the attack instead of resizing or perturbation, we add large Gaussian noises ($\sigma = 9$) to the resized images, and report it as “Ablation”.

We choose 8 typical detectors ranging from the first end-to-end detector to recent ones for attack and test. The variety of models guarantees the validity of results. We specify their information in Table 3 and the corresponding pre-processing or details in Appendix C.

Table 3: Model backbone and mAPs

ID	Model	Backbone	mAP
M1	SSD512 [46]	VGG16	29.3
M2	YOLOv3 [40]	Darknet	33.4
M3	RetinaNet [47]	ResNet-101	38.1
M4	Faster R-CNN [48]	ResNeXt-101-64*4d	40.7
M5	Mask R-CNN [44]	ResNeXt-101-64*4d	42.1
M6	Cascade RCNN [49]	ResNet-101	42.5
M7	Cascade Mask R-CNN [49]	ResNeXt-101-64*4d	45.7
M8	Hyrbrid Task Cascade [45]	ResNeXt-101-64*4d	46.9
M9	EfficientDet [50]	EfficientNet + BiFPN	53.9

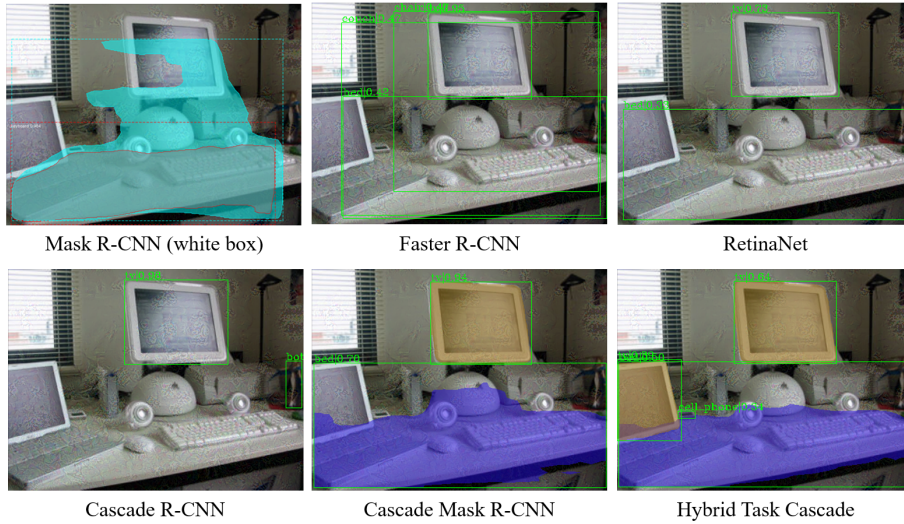


Figure 6: RAD has a great transferability. The same adversarial sample generated by attacking Mask R-CNN fools all 5 black-box detectors.

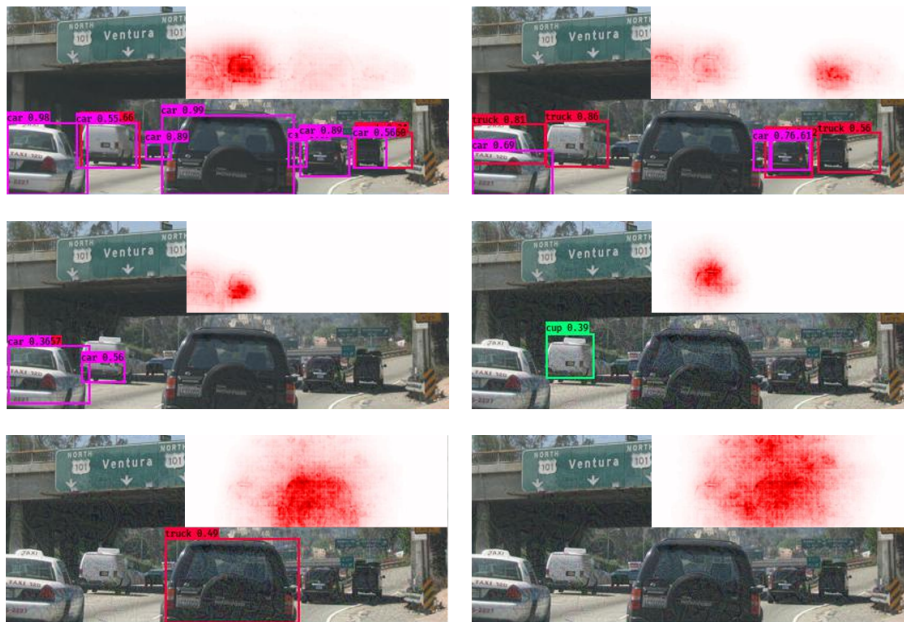


Figure 7: Transition of prediction and relevance map in RAD (from top to bottom and left to right).

4.2. Visual Results of RAD

We first intuitively illustrate the attack process in Fig. 7 and transferability in Fig. 6.

By RAD, the relevance map is attacked to be meaningless and loses its focus. In Fig. 7, the initial prediction is correct and the relevance map is clear. RAD constantly misleads the relevance map to be unstructured without the outline of objects. Finally, all bounding boxes vanish.

In Fig. 6, we visualize several predictions on the same adversarial sample by black-box models. The objects in the image, e.g., the laptop and keyboard, are quite large and obvious to detect. However, with a small perturbation from RAD, 5 black-box models all fail to detect the laptop, keyboard, and mouse. Surprisingly, 4 of them even detect a non-existent “bed”, which is neither relevant nor similar in the image.

4.3. RAD’s Transferability in Object Detection

To evaluate the in-domain transferability of detection attacks and cross-domain transferability of classification attacks, we test the detection mAP of 8 models in COCO adversarial samples generated in the same setting.

For detection attacks, adversarial samples are crafted by attacking surrogate model M2 (YOLOv3 [40]). For classification attacks, we use the model output on the clean sample as the label. By several state-of-the-art attacks on surrogate classifiers (InceptionV3 [51] here as in [10, 20]), the adversarial samples are generated and tested the mAP as the transferability towards detectors. Details of implementation are described in Appendix C.

We present the results in Table 4. Among the classification attacks and detection ones, cross-domain attack [52] is effective, but RAD is more aggressive. RAD enjoys a state-of-the-art transferability towards most black-box models, outperforming other methods for above 20%. The detection mAPs are more than halved, making state-of-the-art detectors similar to the early single-shot detector (YOLO, M2).

Method	M1	M2	M3	M4	M5	M6	M7	M8	M9
No Attack	29.3	33.4	38.1	40.7	42.1	42.5	45.7	46.9	53.9
Ablation	24.9	31.4	31.2	31.6	35.0	34.3	37.5	38.8	48.6
PGD	26.4	30.4	34.4	35.4	38.4	38.3	41.7	43.1	51.1
SI-PGD	27.5	31.6	36.1	37.1	40.0	40.1	43.5	44.8	52.4
MI-DI-PGD	22.9	26.2	29.3	30.0	33.2	32.1	36.0	37.5	48.0
MI-TI-PGD	20.1	23.7	24.9	25.4	30.1	27.4	32.8	34.5	47.1
CD-painting	16.4	20.8	21.3	22.8	26.6	24.5	28.9	29.5	42.3
CD-comics	16.6	21.6	21.7	22.7	26.8	24.3	29.1	42.3	43.7
Dfool	23.3	2.5	29.2	29.8	33.3	32.9	36.5	38.0	47.5
Loc	21.9	0.2	25.8	26.6	29.8	29.4	33.2	33.2	45.2
DAG	20.8	0.6	22.8	23.4	26.8	25.6	28.9	31.0	40.6
RAD	14.6	0.7	16.3	17.0	20.4	19.1	22.3	23.8	35.0

The influence of ε on detection mAP in RAD are displayed in Fig. 8. With the ℓ_∞ bound increases, the resulting mAP greatly decreases for all black-box models especially for ε from 8 to 12.

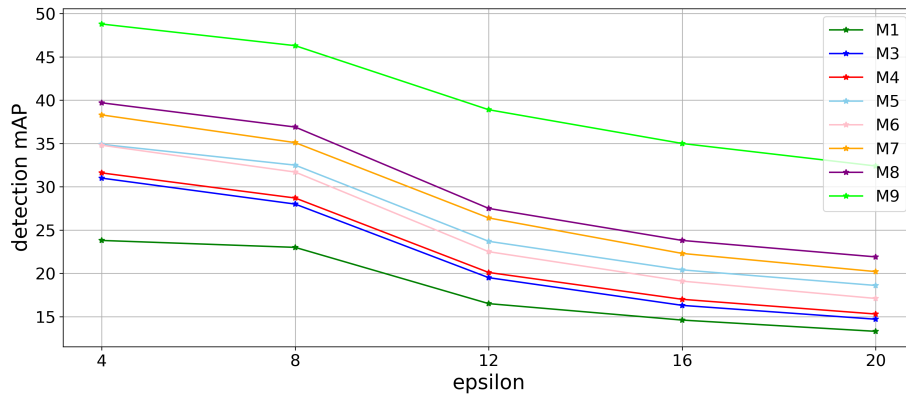


Figure 8: The influence of ε on detection mAP in RAD

4.4. RAD’s Transferability to Instance Segmentation

Detection and segmentation are similar in some aspects, so they could be implemented in one network [44, 49, 45]. Also, adversarial samples for object detection tend to transfer to instance segmentation [16]. Accordingly, we evaluate this cross-task transferability by RAD on surrogate detectors YOLOv3 ([40], M2), RetinaNet ([47], M3) and Mask R-CNN ([44], M5). From the results in Table 5, we find that RAD also greatly hurts the performance of instance segmentation, leading to a drop in mAP of over 70%. This inspires the segmentation attackers to indirectly attack detectors.

Table 5: Segmentation mAP of RAD

Surrogate	mAP			mAP50			mAP75		
	M5	M7	M8	M5	M7	M8	M5	M7	M8
None	38.0	39.4	40.8	60.6	61.3	63.3	40.9	42.9	44.1
Ablation	31.0	31.9	33.5	51.2	51.0	53.7	32.4	34.3	35.4
M2	17.9	18.6	20.3	31.6	31.7	34.5	18.0	18.9	20.7
M3	11.6	11.9	12.9	19.2	19.1	20.7	12.1	12.6	13.7
M5	1.2	11.1	11.8	2.4	17.9	18.9	1.0	11.9	12.6

5. Adversarial Objects in Context

Given the great transferability of RAD, we create Adversarial Objects in COntext (AOCO), the first adversarial dataset for object detection and instance segmentation. AOCO dataset serves as a potential benchmark to evaluate the robustness of detectors, which will be beneficial to network designers. It will also be useful for adversarial training, as the most effective practice to improve the robustness of DNNs [53, 54]. Notice that there is no other adversarial dataset for detection and segmentation at all. This is not because the dataset is useless, but due to the low transferability of attack methods such that the examples are detector-dependent. Now we have achieved high transferability and can then make such an adversarial dataset publicly available.

AOCO is generated from the full COCO 2017 validation set [23] with 5k samples. It contains 5K adversarial samples for evaluating object detection (AOCO detection) and 5K for instance segmentation (AOCO segmentation). All 10K samples in AOCO are crafted by RAD. The surrogate model we attack is YOLOv3 for AOCO detection and Mask R-CNN for AOCO segmentation given the results in Table 4 and Table 5.

We measure the perturbation Δx in AOCO by Root Mean Squared Error (RMSE) as in [16, 55]. It is calculated as $\sqrt{\sum_i (\Delta x_i)^2 / N}$ in a pixel-wise way, and N is the size of the image. Performance of AOCO is reported in Table 6. The RMSE in AOCO is 6.469 for detection and 6.606 for segmentation, which is lower than that in [56], and the perturbations are quite imperceptible. We show in Fig. 9 the AOCO samples. More details are presented in Appendix D.

Table 6: Detection mAP and segmentation mAP on COCO and AOCO

	M1	M2	M3	M4	M5	M6	M7	M8	M9
COCO det.	29.3	33.4	38.1	40.7	42.1	42.5	45.7	46.9	53.9
AOCO det.	14.6	0.7	16.3	17	20.4	19.1	22.3	23.8	35.0
COCO seg.	\	\	\	\	38.0	\	39.4	40.8	\
AOCO seg.	\	\	\	\	1.2	\	11.1	11.8	\

6. Conclusion

To pursue a high transferability, this paper proposes Relevance Attack on Detectors (RAD), which works by suppressing the multi-node relevance, a common property across detectors calculated by our Multi-Node SGLRP. We also thoroughly discuss where to attack and how to update in attacking relevance maps. RAD achieves a state-of-the-art transferability towards 8 diverse black-box models, exceeding existing results by above 20%, and also significantly hurts the instance segmentation. Given the great transferability of RAD, we generate the first adversarial dataset for object detection and instance segmentation, i.e.,

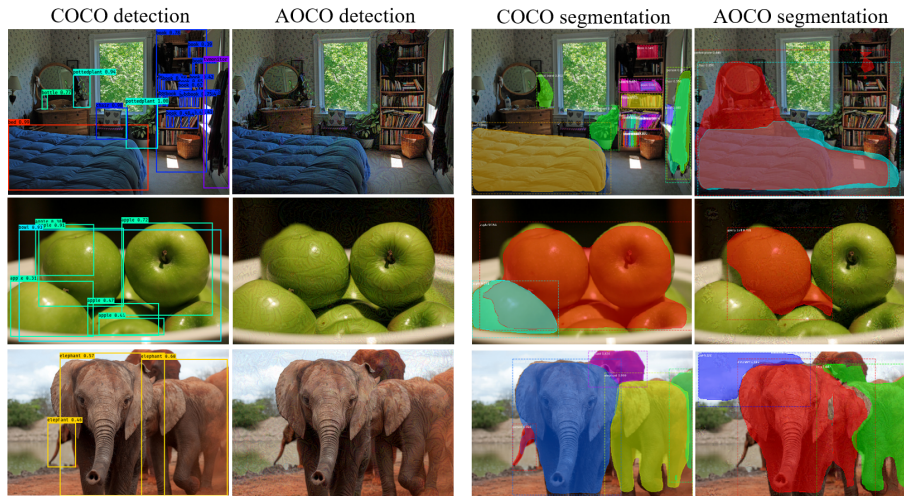


Figure 9: Detection and segmentation results in COCO and AOCO by YOLOv3 and Mask R-CNN. For COCO, both networks predict correctly. For AOCO segmentation results, the top image contains two big masks for “chair” and “potted plant”; the second image contains one false mask for “sports ball”; the bottom image contains “dog” in green, “car” in purple and “elephant” in red.

Adversarial Objects in Context (AOCO), which helps to quickly evaluate and improve the robustness of detectors. Also, attacking other common properties is promising for good transferability.

7. Acknowledgments

This work was partially supported by National Key Research Development Project (No. 2018AAA0100702), National Natural Science Foundation of China (No. 61977046), and 1000-Talent Plan (Young Program).

References

- [1] C. Szegedy, W. Zaremba, I. Sutskever, J. Bruna, D. Erhan, I. J. Goodfellow, R. Fergus, Intriguing properties of neural networks, in: 2nd International Conference on Learning Representations, ICLR, 2014.

- [2] I. J. Goodfellow, J. Shlens, C. Szegedy, Explaining and harnessing adversarial examples, in: *STAT*, Vol. 1050, 2015, p. 20.
- [3] N. Carlini, D. Wagner, Towards evaluating the robustness of neural networks, in: *2017 IEEE Symposium on Security and Privacy (SP)*, IEEE, 2017, pp. 39–57.
- [4] A. Mađry, A. Makelov, L. Schmidt, D. Tsipras, A. Vladu, Towards deep learning models resistant to adversarial attacks, *STAT 1050* (2017) 9.
- [5] S. Baluja, I. Fischer, Adversarial transformation networks: Learning to generate adversarial examples, arXiv preprint arXiv:1703.09387.
- [6] J. Su, D. V. Vargas, K. Sakurai, One pixel attack for fooling deep neural networks, in: *IEEE Transactions on Evolutionary Computation*, IEEE, 2019.
- [7] N. Papernot, P. McDaniel, I. Goodfellow, Transferability in machine learning: from phenomena to black-box attacks using adversarial samples, arXiv preprint arXiv:1605.07277.
- [8] W. Brendel, J. Rauber, M. Bethge, Decision-based adversarial attacks: Reliable attacks against black-box machine learning models, in: *6th International Conference on Learning Representations, ICLR*, 2018.
- [9] Y. Dong, F. Liao, T. Pang, H. Su, J. Zhu, X. Hu, J. Li, Boosting adversarial attacks with momentum, in: *Proceedings of the IEEE Conference on Computer Vision and Pattern Recognition*, 2018, pp. 9185–9193.
- [10] C. Xie, Z. Zhang, Y. Zhou, S. Bai, J. Wang, Z. Ren, A. L. Yuille, Improving transferability of adversarial examples with input diversity, in: *Proceedings of the IEEE Conference on Computer Vision and Pattern Recognition*, 2019, pp. 2730–2739.
- [11] J. Lin, C. Song, K. He, L. Wang, J. E. Hopcroft, Nesterov accelerated gradient and scale invariance for adversarial attacks, in: *8th International Conference on Learning Representations, ICLR*, 2020.

- [12] S. Chen, Z. He, C. Sun, X. Huang, Universal adversarial attack on attention and the resulting dataset damagenet, in: *IEEE Transactions on Pattern Analysis and Machine Intelligence*, 2020.
- [13] H. Zhang, J. Wang, Towards adversarially robust object detection, in: *Proceedings of the IEEE International Conference on Computer Vision*, 2019, pp. 421–430.
- [14] S. Thys, W. Van Ranst, T. Goedemé, Fooling automated surveillance cameras: adversarial patches to attack person detection, in: *Proceedings of the IEEE Conference on Computer Vision and Pattern Recognition Workshops*, 2019.
- [15] D. Su, H. Zhang, H. Chen, J. Yi, P.-Y. Chen, Y. Gao, Is robustness the cost of accuracy?—a comprehensive study on the robustness of 18 deep image classification models, in: *Proceedings of the European Conference on Computer Vision (ECCV)*, 2018.
- [16] C. Xie, J. Wang, Z. Zhang, Y. Zhou, L. Xie, A. Yuille, Adversarial examples for semantic segmentation and object detection, in: *Proceedings of the IEEE International Conference on Computer Vision*, 2017, pp. 1369–1378.
- [17] Y. Li, D. Tian, X. Bian, S. Lyu, et al., Robust adversarial perturbation on deep proposal-based models, in: *British Machine Vision Conference, BMVC*, 2018.
- [18] Y. Li, X. Bian, M.-C. Chang, S. Lyu, Exploring the vulnerability of single shot module in object detectors via imperceptible background patches, in: *British Machine Vision Conference, BMVC*, 2019.
- [19] Y. Li, X. Bian, S. Lyu, Attacking object detectors via imperceptible patches on background, *CoRR*, abs/1809.05966.
- [20] Y. Dong, T. Pang, H. Su, J. Zhu, Evading defenses to transferable adversarial examples by translation-invariant attacks, in: *Proceedings of the IEEE*

- Conference on Computer Vision and Pattern Recognition, 2019, pp. 4312–4321.
- [21] T. Zhang, Z. Zhu, Interpreting adversarially trained convolutional neural networks, in: Proceedings of the 36th International Conference on Machine Learning, ICML, 2019, pp. 7502–7511.
- [22] W. Wu, Y. Su, X. Chen, S. Zhao, I. King, M. R. Lyu, Y.-W. Tai, Boosting the transferability of adversarial samples via attention, in: Proceedings of the IEEE/CVF Conference on Computer Vision and Pattern Recognition, 2020, pp. 1161–1170.
- [23] T.-Y. Lin, M. Maire, S. Belongie, J. Hays, P. Perona, D. Ramanan, P. Dollár, C. L. Zitnick, Microsoft coco: Common objects in context, in: Proceedings of the European Conference on Computer Vision (ECCV), Springer, 2014, pp. 740–755.
- [24] N. Papernot, P. McDaniel, I. Goodfellow, S. Jha, Z. B. Celik, A. Swami, Practical black-box attacks against machine learning, in: Proceedings of the 2017 ACM on Asia Conference on Computer and Communications Security, ACM, 2017, pp. 506–519.
- [25] J. Lu, H. Sibai, E. Fabry, Adversarial examples that fool detectors, arXiv preprint arXiv:1712.02494.
- [26] Y. Wang, Y.-a. Tan, W. Zhang, Y. Zhao, X. Kuang, An adversarial attack on dnn-based black-box object detectors, in: Journal of Network and Computer Applications, Elsevier, 2020, p. 102634.
- [27] L. Huang, C. Gao, Y. Zhou, C. Xie, A. L. Yuille, C. Zou, N. Liu, Universal physical camouflage attacks on object detectors, in: Proceedings of the IEEE/CVF Conference on Computer Vision and Pattern Recognition, 2020, pp. 720–729.
- [28] Z. Wu, S.-N. Lim, L. S. Davis, T. Goldstein, Making an invisibility cloak: Real world adversarial attacks on object detectors, in: Proceedings of the

- European Conference on Computer Vision (ECCV), Springer, 2020, pp. 1–17.
- [29] K. Xu, G. Zhang, S. Liu, Q. Fan, M. Sun, H. Chen, P.-Y. Chen, Y. Wang, X. Lin, Adversarial t-shirt! evading person detectors in a physical world, in: Proceedings of the European Conference on Computer Vision (ECCV), Springer, 2020, pp. 665–681.
- [30] Y. Zhang, F. Wang, W. Ruan, Fooling object detectors: Adversarial attacks by half-neighbor masks, arXiv preprint arXiv:2101.00989.
- [31] M. D. Zeiler, R. Fergus, Visualizing and understanding convolutional networks, in: Proceedings of the European Conference on Computer Vision (ECCV), Springer, 2014, pp. 818–833.
- [32] R. R. Selvaraju, M. Cogswell, A. Das, R. Vedantam, D. Parikh, D. Batra, Grad-cam: Visual explanations from deep networks via gradient-based localization, in: Proceedings of the IEEE International Conference on Computer Vision, 2017, pp. 618–626.
- [33] A. Shrikumar, P. Greenside, A. Kundaje, Learning important features through propagating activation differences, in: Proceedings of the 34th International Conference on Machine Learning-Volume 70, JMLR. org, 2017, pp. 3145–3153.
- [34] S. Bach, A. Binder, G. Montavon, F. Klauschen, K.-R. Müller, W. Samek, On pixel-wise explanations for non-linear classifier decisions by layer-wise relevance propagation, in: PloS one, Vol. 10, Public Library of Science, 2015.
- [35] J. Gu, Y. Yang, V. Tresp, Understanding individual decisions of cnns via contrastive backpropagation, in: Asian Conference on Computer Vision, Springer, 2018, pp. 119–134.
- [36] B. K. Iwana, R. Kuroki, S. Uchida, Explaining convolutional neural networks using softmax gradient layer-wise relevance propagation, in: IEEE/CVF

International Conference on Computer Vision Workshops, ICCV Workshops, 2019.

- [37] A. Ghorbani, A. Abid, J. Zou, Interpretation of neural networks is fragile, in: Proceedings of the AAAI Conference on Artificial Intelligence, Vol. 33, 2019, pp. 3681–3688.
- [38] X. Zhang, N. Wang, H. Shen, S. Ji, X. Luo, T. Wang, Interpretable deep learning under fire, in: 29th USENIX Security Symposium, 2020.
- [39] M. Alber, S. Lapuschkin, P. Seegerer, M. Hägele, K. T. Schütt, G. Montavon, W. Samek, K.-R. Müller, S. Dähne, P.-J. Kindermans, investigate neural networks, in: Journal of Machine Learning Research, Vol. 20, 2019, pp. 1–8.
- [40] J. Redmon, A. Farhadi, Yolov3: An incremental improvement, arXiv preprint arXiv:1804.02767.
- [41] F. Chollet, et al., Keras, <https://keras.io> (2015).
- [42] M. Abadi, A. Agarwal, P. Barham, E. Brevdo, Z. Chen, C. Citro, G. S. Corrado, A. Davis, J. Dean, M. Devin, S. Ghemawat, I. Goodfellow, A. Harp, G. Irving, M. Isard, Y. Jia, R. Jozefowicz, L. Kaiser, M. Kudlur, J. Levenberg, D. Mané, R. Monga, S. Moore, D. Murray, C. Olah, M. Schuster, J. Shlens, B. Steiner, I. Sutskever, K. Talwar, P. Tucker, V. Vanhoucke, V. Vasudevan, F. Viégas, O. Vinyals, P. Warden, M. Wattenberg, M. Wicke, Y. Yu, X. Zheng, TensorFlow: Large-scale machine learning on heterogeneous systems, software available from tensorflow.org (2015).
URL <https://www.tensorflow.org/>
- [43] A. Paszke, S. Gross, F. Massa, A. Lerer, J. Bradbury, G. Chanan, T. Killeen, Z. Lin, N. Gimelshein, L. Antiga, et al., Pytorch: An imperative style, high-performance deep learning library, in: Advances in Neural Information Processing Systems, 2019, pp. 8024–8035.
- [44] K. He, G. Gkioxari, P. Dollár, R. Girshick, Mask R-CNN, in: Proceedings of the IEEE international conference on computer vision, 2017, pp. 2961–2969.

- [45] K. Chen, J. Pang, J. Wang, Y. Xiong, X. Li, S. Sun, W. Feng, Z. Liu, J. Shi, W. Ouyang, et al., Hybrid task cascade for instance segmentation, in: Proceedings of the IEEE Conference on Computer Vision and Pattern Recognition, 2019, pp. 4974–4983.
- [46] W. Liu, D. Anguelov, D. Erhan, C. Szegedy, S. Reed, C.-Y. Fu, A. C. Berg, Ssd: Single shot multibox detector, in: Proceedings of the European Conference on Computer Vision (ECCV), Springer, 2016, pp. 21–37.
- [47] T.-Y. Lin, P. Goyal, R. Girshick, K. He, P. Dollár, Focal loss for dense object detection, in: Proceedings of the IEEE international conference on computer vision, 2017, pp. 2980–2988.
- [48] S. Ren, K. He, R. Girshick, J. Sun, Faster r-cnn: Towards real-time object detection with region proposal networks, in: Advances in Neural Information Processing Systems, 2015, pp. 91–99.
- [49] Z. Cai, N. Vasconcelos, Cascade r-cnn: Delving into high quality object detection, in: Proceedings of the IEEE Conference on Computer Vision and Pattern Recognition, 2018, pp. 6154–6162.
- [50] M. Tan, R. Pang, Q. V. Le, Efficientdet: Scalable and efficient object detection, in: Proceedings of the IEEE/CVF Conference on Computer Vision and Pattern Recognition, 2020, pp. 10781–10790.
- [51] C. Szegedy, V. Vanhoucke, S. Ioffe, J. Shlens, Z. Wojna, Rethinking the inception architecture for computer vision, in: Proceedings of the IEEE Conference on Computer Vision and Pattern Recognition, 2016, pp. 2818–2826.
- [52] M. M. Naseer, S. H. Khan, M. H. Khan, F. S. Khan, F. Porikli, Cross-domain transferability of adversarial perturbations, in: Advances in Neural Information Processing Systems, 2019, pp. 12905–12915.

- [53] D. Zhang, T. Zhang, Y. Lu, Z. Zhu, B. Dong, You only propagate once: Painless adversarial training using maximal principle, in: Advances in Neural Information Processing Systems 32, 2019, pp. 227–238.
- [54] F. Tramèr, A. Kurakin, N. Papernot, I. J. Goodfellow, D. Boneh, P. D. McDaniel, Ensemble adversarial training: Attacks and defenses, in: 6th International Conference on Learning Representations, ICLR, 2018.
- [55] Y. Liu, X. Chen, C. Liu, D. Song, Delving into transferable adversarial examples and black-box attacks, in: Proceedings of 5th International Conference on Learning Representations, 2017.
- [56] D. Wu, Y. Wang, S. Xia, J. Bailey, X. Ma, Skip connections matter: On the transferability of adversarial examples generated with resnets, in: 7th International Conference on Learning Representations, ICLR, 2019.

Appendix A. Relevance Back-Propagation Rules (DTD)

DTD-based interpreters, such as LRP, CLRP, and SGLRP, back-propagate the relevance from the output layer to the input layer according to the rules specified in this section. Their only difference is the relevance in the initial output layer $R_n^{(L)}$.

For each layer l in a DNN with L layers in total, suppose layer l has N nodes and layer $l + 1$ has M nodes, the relevance $R_n^{(L)}$ at node n in layer l is defined recursively by

$$R_n^{(l)} = \sum_m \frac{a_n^{(l)} w_{n,m}^{+(l)}}{\sum_{n'} a_{n'}^{(l)} w_{n',m}^{+(l)}} R_m^{(l+1)},$$

for nodes with definite positive values (such as after ReLU), and

$$R_n^{(l)} = \sum_m \frac{z_n^{(l)} w_{n,m}^{(l)} - b_n^{(l)} w_{n,m}^{+(l)} - h_n^{(l)} w_{n,m}^{-(l)}}{\sum_{n'} \frac{z_{n'}^{(l)} w_{n',m}^{(l)} - b_{n'}^{(l)} w_{n',m}^{+(l)} - h_{n'}^{(l)} w_{n',m}^{-(l)}}{z_{n'}^{(l)} w_{n',m}^{(l)} - b_{n'}^{(l)} w_{n',m}^{+(l)} - h_{n'}^{(l)} w_{n',m}^{-(l)}}} R_m^{(l+1)},$$

for nodes that may have negative values. In the formulas above, $a_n^{(l)}$ is the post-activation output of node n in layer l and $z_n^{(l)}$ is the pre-activation one. The range $[b_n^{(l)}, h_n^{(l)}]$ stands for the minimum and maximum of $z_n^{(l)}$. Finally, $w_{n,m}^{+(l)} = \max(w_{n,m}^{(l)}, 0)$ and $w_{n,m}^{-(l)} = \min(w_{n,m}^{(l)}, 0)$.

According to the propagation rules above as mentioned in [36], we could naturally obtain the attack gradients as

$$\frac{\partial R_m^{(l+1)}}{\partial R_n^{(l)}} = \begin{cases} \left(\sum_m \frac{a_n^{(l)} w_{n,m}^{+(l)}}{\sum_{n'} a_{n'}^{(l)} w_{n',m}^{+(l)}} \right)^{-1}, & \text{for nodes with definite positive values} \\ \left(\sum_m \frac{z_n^{(l)} w_{n,m}^{(l)} - b_n^{(l)} w_{n,m}^{+(l)} - h_n^{(l)} w_{n,m}^{-(l)}}{\sum_{n'} \frac{z_{n'}^{(l)} w_{n',m}^{(l)} - b_{n'}^{(l)} w_{n',m}^{+(l)} - h_{n'}^{(l)} w_{n',m}^{-(l)}}{z_{n'}^{(l)} w_{n',m}^{(l)} - b_{n'}^{(l)} w_{n',m}^{+(l)} - h_{n'}^{(l)} w_{n',m}^{-(l)}}} \right)^{-1}, & \text{otherwise} \end{cases}.$$

Appendix B. Influence of Hyper-Parameters in Node Selection

Performance of RAD is not sensitive to hyper-parameter, no matter the strategy to select bounding boxes is dynamic or static as Table B.7. Attackers are not bothered to tune them carefully. The parameter for dynamic strategy refers to the pre-softmax confidence threshold to select a bounding box. The parameter for static strategy refers to the fixed number of selected bounding boxes in each iteration.

Table B.7: Detection mAP in different hyper-parameters in RAD

Str.	Para.	M1	M2	M3	M4	M5	M6	M7	M8	M9
Dyn.	-1	18.3	1.2	20.0	20.6	24.3	22.8	26.7	28.3	40.0
	-2	18.2	1.2	20.1	20.7	24.2	22.8	26.6	28.0	39.8
	-3	18.4	1.3	20.3	20.8	24.3	22.9	26.7	28.5	40.2
Sta.	10	18.2	1.1	19.9	20.5	24.2	22.8	26.2	28.0	39.8
	20	18.1	1.2	19.9	20.5	24.3	22.6	26.4	28.2	39.9
	30	18.2	1.3	20.1	20.7	24.3	22.8	26.0	27.9	40.1

Appendix C. Implementation Details

Appendix C.1. Pre-processing

To pre-process, we resize the image with its long side as 416 for YOLOv3 or RetinaNet and 448 for Mask R-CNN, and then zero-pad it to a square. The resolution is kept relatively the same for a fair evaluation. Images are normalized to $[0,1]$ in YOLOv3 or subtracted by the mean of COCO training set in RetinaNet and Mask R-CNN. Accordingly, samples in AOCO detection have the long side 416, and that for AOCO segmentation is 448.

Appendix C.2. Transfer-Enhancing Update Techniques

DI [10] transforms the image for 4 times with probability p ($p = 1$ for better transferability as suggested) and averaging the gradients. The transformation is to resize the image to $0.9\times$ its size and randomly padding the outer areas with white pixels. SI [11] divides the sample numerically by the power 2 for 4 times and averages the 4 obtained gradients. TI [20] translates the image to calculate the augmented gradients. To implement it efficiently, it adopts a kernel to simulate the averaging of gradients. We choose the kernel size 15 as suggested. MI [9] uses momentum optimization (parameter $\mu = 1$ as suggested) for a better transferability and a faster attack. Cross-domain attack [52] uses extra datasets (paintings, denoted as CD-paintings, and comics, denoted as CD-comics) to train

a perturbation generator with the relative loss. The adopted surrogate model is also InceptionV3 for consistency. Perturbations are resized to fit the sample size.

Appendix C.3. Detection Attacks

For DAG [16], we follow the setting of generating dense proposals. The classification probabilities of 3000 bounding boxes with the highest confidence are attacked. But we alter its optimization to (5) because its original update produces quite a small perturbation, leading to a poor transferability, which is unfair for comparison. Dfool [25] suppresses the classification confidence for the original bounding boxes, which is the same in our experiment. Localization loss is shown to be useful in [13], and here we suppress the width and height of the original bounding boxes.

Appendix D. More about AOCO

We report the mAP50 and mAP75 of AOCO in Table D.8 and Table D.9.

Table D.8: Detection mAP50 and segmentation mAP50 on COCO and AOCO

	M1	M2	M3	M4	M5	M6	M7	M8	M9
COCO det.	49.2	56.4	58.1	62.0	63.8	60.7	64.1	66.0	74.3
AOCO det.	26.7	1.6	27.6	29.1	34.5	29.9	34.3	37.4	51.7
COCO seg.	\	\	\	\	60.6	\	61.3	63.3	\
AOCO seg.	\	\	\	\	2.4	\	17.9	18.9	\

Table D.9: Detection mAP75 and segmentation mAP75 on COCO and AOCO

	M1	M2	M3	M4	M5	M6	M7	M8	M9
COCO det.	30.8	35.8	40.6	44.6	46.3	46.3	50.0	51.2	59.9
AOCO det.	14.2	0.6	16.5	17.1	20.8	19.9	23.3	24.6	37.4
COCO seg.	\	\	\	\	40.9	\	42.9	44.1	\
AOCO seg.	\	\	\	\	1.0	\	11.9	12.6	\